Newcastle University

ePrints

**Gao X, Zhang J, Yang F, Shang C, Huang D.**

**Robust Proportional–Integral–Derivative (PID) Design for Parameter Uncertain Second-Order Plus Time Delay (SOPTD) Processes Based on Reference Model Approximation.**

***Industrial & Chemical Engineering Research* 2017, 56(41), 11903-11918.**

**Copyright:**

This document is the Accepted Manuscript version of a Published Work that appeared in final form in Industrial & Chemical Engineering Research, copyright © American Chemical Society after peer review and technical editing by the publisher. To access the final edited and published work see:

https://doi.org/10.1021/acs.iecr.7b03155

**Date deposited:**

25/10/2017

**Embargo release date:**

24 September 2018

**Newcastle University ePrints - eprint.ncl.ac.uk**

# Robust PID Design for Parameter Uncertain SOPTD Processes Based on Reference Model Approximation

**Xinqing Gao [a,b], Jie Zhang [c], Fan Yang [a,b], Chao Shang [a,b], Dexian Huang [a,b,*]**

[a] Department of Automation, Tsinghua University, Beijing 100084, China

[b] Tsinghua National Laboratory for Information Science and Technology, Beijing 100084, China

[c] School of Chemical Engineering and Advanced Materials, Newcastle University, Newcastle NE1 7RU, UK

## Abstract

To design robust PID controllers for second-order plus time delay (SOPTD) processes with parameter uncertainty, a reference model approximation method is proposed in this study. The central idea is to enable the frequency response of the PID controller to approximate that of a user-specified reference model. A convex hull is utilized to approximate the frequency template of the parameter uncertain process, and the maximum approximation error of the reference model among all candidate processes is bounded. To guarantee that the PID controller can well shape the closed-loop response of each candidate model to the reference model, a convex optimization problem is formulated to compute the PID parameters by minimizing the upper bound of the approximation error. Constraints on the closed-loop maximum sensitivity peak are imposed on the reference-model approximation problem for loop robustness. The proposed method is able to ensure balanced tracking performance and

[*] Corresponding author at: Department of Automation, Tsinghua University,
E-mail address: huangdx@tsinghua.edu.cn.

disturbance rejection performance through a proper specification of the reference model, and illustrative examples are presented to demonstrate the applicability.

**Keywords**

PID controller, parameter uncertainty, reference model approximation, model-reference control

## 1. INTRODUCTION

Proportional-integral-derivative (PID) controllers are the most extensive controllers in the process industries. In a recent investigation, it has been reported that more than 90% of industrial controllers are of the PID type.[1] The PID controllers have relatively simpler control structures and more understood principles compared to advanced control techniques, and meanwhile the control performance is usually satisfactory or acceptable in most scenarios. These features are the main reasons for the widespread popularity of PID controllers. With the availability of the process models, PID parameters can be derived either by analytic rules, such as the Ziegler-Nichols (Z-N) method[2, 3] and the internal-model-control (IMC) method,[4-6] or by optimization methods in terms of certain control objectives.[7, 8] Even though most controlled processes have higher-order dynamics, it should be noted that the dynamics is usually slow, and the dynamic feature in the lower frequency range is of more concern. Because the process dynamics induced by small poles can usually be neglected, a majority of stable controlled processes can be well approached by simplified and stable first-order plus time delay (FOPTD) models or second-order plus time delay (SOPTD) models.[9, 10] Moreover, a significant number of practical PID design methods are based on these simplified models as well.[11-13]

The performance of model-based controllers is highly related to the model accuracy, yet model uncertainty is inevitable because an extremely accurate process model is difficult to obtain in practice. The FOPTD or SOPTD models are usually built based on identification experiments,[14, 15] yet the identification error in the presence of stochastic noise and disturbances is unavoidable, which would further bring in model uncertainty in the stage of process modeling. In addition, the process nonlinearity is another critical cause for the model uncertainty. Most industrial processes are nonlinear, and linear process models can only approximate the process dynamics at a specific operating point. Since operating point changes are common in practice, a single linear model can hardly well represent the dynamics of nonlinear processes with varying operating points.[16] The parameter uncertainty representation is a widely applied description of model uncertainty in practice due to the clear physical meaning, which assumes that the controlled process has uncertain but bounded parameters. The parameter bound can be estimated through model uncertainty analysis in the framework of system identification, or obtained by including local models at different operating points. Robust PID design and performance monitoring techniques aimed at possible plant model mismatch is a demanding issue to accommodate practical applications. The resulting PID controllers guarantee satisfactory performance in the presence of operating condition changes, and meanwhile the corresponding performance benchmark, which serves as a reference for detecting control performance degradation, is also more reasonable and accessible than single linear-model based benchmarks.[17] A significant number of PID design methods for parameter uncertainty are based on the Kharitonov's theorem that investigates the stability region of interval processes (with fixed delays).[18] The Kharitonov region in the PID parameter space is

computed, which is the set of PID parameters stabilizing the parameter uncertain processes.[19, 20] Nevertheless, it should be noted that the Kharitonov theorem does not directly address the control performance issues for PID design. Another drawback of the Kharitonov-based methods is that they can hardly deal with the uncertainty of time delay. A more easily implemented method in practice is to resort to the conventional model-based PID for the nominal model such as the IMC-PID,[21] and the parameter uncertainty issue is accommodated by adopting a proper IMC filter to increase the loop robustness. Yet in cases where the cancelled poles are overly slow compared to the dominant pole, the response to disturbance may be sluggish and the disturbance rejection performance is not satisfactory in general.[22]

The PID design for parameter uncertain FOPTD processes has already been addressed in our previous work[10], where the PID controller is designed by directly minimizing the worst-case integrated squared error (ISE) subject to step set-point changes and the resulting robust PID is further utilized to establish an accessible performance benchmark for controller performance assessment. Despite the fact that FOPTD models are often reasonable and simple approximations of the controlled processes, there are still some processes with more complicated dynamics and are not suitable to be approximated by FOPTD models, and hence SOPTD models may be more reasonable approximations in such scenarios. Another issue of the method in that paper[10] is the computational burden. The involved optimization problem is nonlinear and nonconvex, and the PID parameters are optimized by brutal grid search. Even though some simplifications have been applied to reduce the computation time, the computational burden is still a concern for practical implementation. To address these issues, a novel reference model approximation method is proposed in this article for parameter

uncertain SOPTD processes. The PID controllers are designed by reference-model approximation, which is different from directly minimizing the ISE. In the spirit of model-reference PID control,[23-26] a reference model is adopted to describe the control objective, which is to enable the set-point response of the PID controller to follow the trajectory of the user-specified reference model. By specifying different types of reference models, the resulting PID can achieve either satisfactory tracking performance or disturbance rejection performance, which is a nice feature of the reference-model based approach. The PID parameters are derived by minimizing the divergence between the frequency response of the closed-loop system and that of the reference model. Even though conventional reference-model based PID design methods are aimed at fixed process models, in this study this kind of approach is extended to parameter uncertain cases. In model uncertain cases, the PID controller is aimed at a set of candidate process models, and a convex hull is established to approximate the frequency template of the parameter uncertain process. By this approach, an upper bound of the maximum approximation error is estimated accordingly, and consequently a convex optimization problem is formulated to derive the PID parameters in the model uncertain case, which is to minimize the upper bound of the maximum approximation error such that the closed-loop trajectory of each possible candidate model can approach that of the reference model. To ensure sufficient stability margin for parameter uncertainty, constraints on the closed-loop maximum sensitivity peak are added to the reference model approximation problem. Such constraints on loop robustness can be relaxed as linear inequality constraints using the standard convex-concave procedure.[27-29] Hence the convexity of the reference model approximation problem is preserved, and the PID

parameters are optimized using iterative convex optimization techniques in a computationally cost efficient way.

The rest of this article is organized as follows. In Section 2, the problem to be solved is formulated. In Section 3, the reference model approximation method of PID controller design for a single linear model is depicted, and related implementation issues are discussed as well. Section 4 presents the reference model approximation method for SOPTD processes with parameter uncertainties. Illustrated examples are given in Section 5 to demonstrate the effectiveness of the proposed method. Some concluding remarks are provided in the final section.

## 2. PROBLEM FORMULATION

In the process industries, the dynamics of a majority of stable controlled processes can be well approximated by stable SOPTD models that are formulated as follows:

$$p(s;\boldsymbol{\theta}) = \frac{K}{T_2 s^2 + T_1 s + 1} e^{-\tau s} \qquad T_1 > 0,\ T_2 \geq 0,\ \tau \geq 0 \tag{1}$$

where $\boldsymbol{\theta} = (K, T_1, T_2, \tau)^T$ is the parameter vector of the SOPTD model $p(s;\boldsymbol{\theta})$. For the parameter uncertain SOPTD model $P(s;\boldsymbol{\Theta})$, it can be viewed as the set of $p(s;\boldsymbol{\theta})$ and is formulated as follows:

$$P(s;\boldsymbol{\Theta}) = \left\{ p(s;\boldsymbol{\theta}) \middle| \begin{matrix} K^- \leq K \leq K^-, T_1^- \leq T_1 \leq T_1^+ \\ T_2^- \leq T_2 \leq T_2^+, \tau^- \leq \tau \leq \tau^+ \end{matrix} \right\} \tag{2}$$

The superscripts "-" and "+" represent the lower and upper bounds of the corresponding model parameter, respectively, and $\boldsymbol{\Theta}$ denotes the set of the process parameter vector $\boldsymbol{\theta}$:

$$\boldsymbol{\Theta} = \left\{ (K, T_1, T_2, \tau)^T \middle| \begin{matrix} K^- \leq K \leq K^-, T_1^- \leq T_1 \leq T_1^+ \\ T_2^- \leq T_2 \leq T_2^+, \tau^- \leq \tau \leq \tau^+ \end{matrix} \right\} \tag{3}$$

Furthermore, it is assumed that the sign of the gain of each model in $P(s;\Theta)$ is the same, and without loss of generality is assumed to be positive.

Consider the following feedback scheme shown in Figure 1.

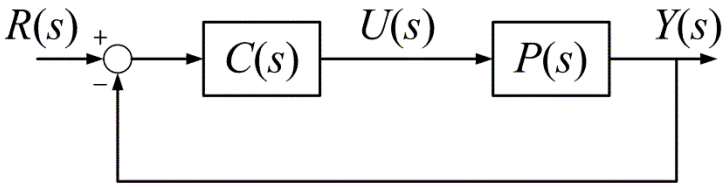


**Figure** 1 The SISO feedback control loop

The closed-loop servo model $T(s)$ from setpoint change $R(s)$ to the process output $Y(s)$ is formulated as:

$$T(s)=\frac{Y(s)}{R(s)}=\frac{P(s)C(s)}{1+P(s)C(s)} \tag{4}$$

In practice, the form of PID controller is usually formulated:

$$C(s)=K_p\left(1+\frac{1}{T_i s}+T_d s\right) \tag{5}$$

where $K_p$, $T_i$ and $T_d$ represent the controller gain, integral time and derivative time, respectively. For simplicity of mathematical formulas, the form of PID controllers in (5) is reformulated as $C(s;\boldsymbol{\beta})=K_p+\frac{K_i}{s}+K_d s$ and $\boldsymbol{\beta}=\left(K_p,K_i,K_d\right)^T$ is the PID parameter vector. Since an explicit linear model is hardly available in practice, we aim at a robust PID controller that can guarantee satisfactory performance for $P(s;\Theta)$ defined in (2). In the spirit of model-reference control, the desired set-point response can be described by a user-specified reference model $T_r(s)$:

$$Y(s)=T_r(s)R(s) \tag{6}$$

The design objective is described as follows:

(1) For each candidate model $p(s;\boldsymbol{\theta})$ in $P(s;\Theta)$, the closed-loop servo model with

the PID controller $C(s)$ is expected to approximate that of a prespecified reference model $T_r(s)$;

(2) The stability margin of $C(s)$ for each candidate model $p(s;\theta)$ should be sufficient to guarantee control loop robustness and operation safety.

# 3. A REFERENCE-MODEL APPROXIMATION METHOD FOR PID CONTROLLER DESIGN

## *3.1 Derivation of PID parameters based on convex optimization*

In this section, a convex optimization problem is formulated to calculate the desired PID controller for a single linear model. The sensitivity function $S(s;\beta)$ of $C(s;\beta)$ can be derived as follows:

$$S(s;\beta)=1-T(s;\beta)=\frac{1}{1+P(s)C(s;\beta)} \tag{7}$$

It is obvious that:

$$T(s;\beta)=P(s)C(s;\beta)S(s;\beta) \tag{8}$$

If $C(s;\beta)$ can guarantee that servo model $T(s;\beta)$ is equivalent to the prespecified reference model $T_r(s)$, the following expression can be arrived:

$$T_r(s)=P(s)C(s;\beta)\left(1-T_r(s)\right) \tag{9}$$

Nevertheless, it is rare that such condition can be fully satisfied, and thus the desired controller can be derived by minimizing the difference between the two sides of (9). This objective formulated in (9) is similar to that of the virtual reference feedback tuning (VRFT) design framework[23-25] in some sense, but the major difference is that a full knowledge of the process model is utilized. It can be seen that the algebraic relation from $\beta$ to $C(s;\beta)$ is affine. A simple yet effective approach to approximation of the transfer functions can rely on

the frequency response:

$$\min_{\boldsymbol{\beta}} J = \left\| \boldsymbol{\Omega} - \boldsymbol{\Phi} \cdot \boldsymbol{\beta} \right\|_2^2 \tag{10}$$

$$\boldsymbol{\Omega} = \left[ T_r\left(j\omega_1\right) \quad T_r\left(j\omega_2\right) \quad \cdots \quad T_r\left(j\omega_N\right) \right]^T \tag{11}$$

$$\boldsymbol{\Phi} = \begin{bmatrix} H_\delta^1\left(j\omega_1\right) & H_\delta^2\left(j\omega_1\right) & H_\delta^3\left(j\omega_1\right) \\ H_\delta^1\left(j\omega_2\right) & H_\delta^2\left(j\omega_2\right) & H_\delta^3\left(j\omega_2\right) \\ \vdots & \vdots & \vdots \\ H_\delta^1\left(j\omega_N\right) & H_\delta^2\left(j\omega_N\right) & H_\delta^3\left(j\omega_N\right) \end{bmatrix} \tag{12}$$

where $H_\delta^1\left(j\omega\right)$, $H_\delta^2\left(j\omega\right)$ and $H_\delta^3\left(j\omega\right)$ are the frequency responses of $P(s)\left(1-T_r(s)\right)$, $P(s)\left(1-T_r(s)\right)/s$ and $P(s)\left(1-T_r(s)\right)s$ respectively, and $T_r\left(j\omega\right)$ is the frequency response of $T_r(s)$. The frequency responses of the involved transfer functions at the frequencies $\omega_i$ $(1 \le i \le N)$ are used for controller design, and $\omega_N$ is the upper bound of the frequency range. In practice, the PID controller usually operates under the ultimate frequency of the controlled process, and $\omega_N$ is specified as:[23]

$$\angle\left[ P\left(j\omega\right) \right]\Big|_{\omega=\omega_N} = -\pi \tag{13}$$

Optimization problem (10) can be reformulated as:

$$\min_{\boldsymbol{\beta}} J = \left\| \tilde{\boldsymbol{\Omega}} - \tilde{\boldsymbol{\Phi}} \cdot \boldsymbol{\beta} \right\|_2^2 \tag{14}$$

$$\tilde{\boldsymbol{\Omega}} = \begin{bmatrix} \mathrm{Re}\left(\boldsymbol{\Omega}\right) \\ \mathrm{Im}\left(\boldsymbol{\Omega}\right) \end{bmatrix}; \tilde{\boldsymbol{\Phi}} = \begin{bmatrix} \mathrm{Re}\left(\boldsymbol{\Phi}\right) \\ \mathrm{Im}\left(\boldsymbol{\Phi}\right) \end{bmatrix} \tag{15}$$

Here, $\mathrm{Re}(\mathbf{X})$ and $\mathrm{Im}(\mathbf{X})$ represent the real matrices with the elements being the real and imaginary parts of the complex matrix $\mathbf{X}$, respectively. Problem (14) can be solved using the least-squares regression:

$$\boldsymbol{\beta}^* = \left( \tilde{\boldsymbol{\Phi}}^T \tilde{\boldsymbol{\Phi}} \right)^{-1} \tilde{\boldsymbol{\Phi}}^T \tilde{\boldsymbol{\Omega}} \tag{16}$$

### *3.2 Specifying the reference model*

For model-reference control, the control objective can be expressed in terms of reference

models. The following first-order reference model is predominantly applied in model-reference control:[30]

$$T_r(s) = \frac{1}{\lambda s + 1} e^{-\tau s} \tag{17}$$

The delay should be set to be equal to the process delay, and the time constant $\lambda$ of the response model determines the response speed with small values yielding faster responses. If a smooth setpoint response without overshoots is required, the reference model in (17) can be adopted for PID design. Yet, the tracking performance can be improved if reasonable overshoots are permitted, and thus the following second-order reference model with slightly underdamping coefficients can be adopted[31]:

$$T_r(s) = \frac{1}{\lambda^2 s^2 + 2\xi\lambda s + 1} e^{-\tau s},\ 0.5 \le \xi \le 1 \tag{18}$$

Through a careful choice of the damping coefficient $\xi$, the response speed can be accelerated compared to the FOPTD reference model, and meanwhile the closed-loop trajectory still remains smooth and the overshoot is acceptable.

The reference models in (17) and (18) can yield smooth set-point responses such that satisfactory tracking performance can be guaranteed. Nevertheless, for controlled processes with slow poles such as lag-dominant processes, the response of input load disturbance would be sluggish for these tunings, and hence the disturbance rejection would be poor. For better disturbance rejection performance, the following reference model can be adopted:[32]

$$\begin{aligned} &T_r(s) = \frac{\alpha s + 1}{\lambda^2 s^2 + 2\xi\lambda s + 1} e^{-\tau s} \\ &0.5 \le \xi \le 1 \end{aligned} \tag{19}$$

The lead part $\alpha s + 1$ can compensate the effect of the slow pole and thus the disturbance

rejection performance is improved. Nevertheless, it must be emphasized the overshoot is increased for this reference model, which means that set-point tracking performance is affected. Since one-degree-of-freedom (1DOF) PID controllers can hardly guarantee the tracking performance and disturbance rejection performance simultaneously, the lead part is desired to be specified depending on the practical requirements on the control objective.

# 4. REFERENCE MODEL ARRPXIMATION FOR SOPTD PROCESSES WITH PARAMATRIC UNCERTAINTY

## *4.1 Optimization criterion of the model approximation problem based on the convex hull of the frequency template*

The primary objective is to design a PID controller that can guarantee reasonable closed-loop responses for all candidate models in $P(s;\Theta)$ despite the parameter uncertainty. Similarly, it is straightforward to describe the control objective in terms of a proper reference model, and hence the PID design is to enable the resulting response of each candidate model in $P(s;\Theta)$ to approach the prespecified reference model as possible. Starting from this motivation, the optimization criterion can be formulated as follows:

$$J(\boldsymbol{\beta}) = \min_{\boldsymbol{\beta}} \left\{ \max_{\boldsymbol{\theta}\in\Theta} \left\| \boldsymbol{\Omega} - \boldsymbol{\Phi}(\boldsymbol{\theta}) \cdot \boldsymbol{\beta} \right\|_2^2 \right\} \tag{20}$$

where the definition of $\boldsymbol{\Omega}$ is the same as that of problem (10) and $\boldsymbol{\Phi}(\boldsymbol{\theta})$ is the frequency response matrix generated via (12) by the candidate SOPTD model $p(s;\boldsymbol{\theta})$ in $P(s;\Theta)$. However, it should be noted that the optimization problem is a bi-level, implying that the computational burden is high. Alternatively, an upper bound of the inner optimization problem can be estimated based on the convex hull that approximates the frequency template $P(j\omega;\Theta)$ of $P(s;\Theta)$. The frequency template $P(j\omega;\Theta)$ is the set of frequency responses

of the candidate models in $P(s;\Theta)$ at frequency $\omega$, which is defined as follows:

$$P(j\omega;\Theta)=\{p(j\omega;\theta)\,|\,\theta\in\Theta\} \tag{21}$$

The optimization objective is altered by minimizing the upper bound of the maximum approximation error such that the computational burden can be reduced.

**Definition 1.** The convex hull of a finite point set $\{v_1,v_2,\ldots,v_n\}$ in the complex plane is the set of all convex combinations of the points in $\{v_1,v_2,\ldots,v_n\}$:

$$\operatorname{conv}\{v_1,v_2,\ldots,v_n\}=\left\{\sum_{i=1}^{n}\lambda_i v_i\,\middle|\,\sum_{i=1}^{n}\lambda_i=1,\lambda_i\geq 0\right\} \tag{22}$$

Each point $v_i\,(i=1,2,\ldots,n)$ is called a vertex of the convex hull $\operatorname{conv}\{v_1,v_2,\ldots,v_n\}$.

**Definition 2.** For the parameter uncertain SOPTD process $P(s;\Theta)$, a convex hull of the frequency template $P(j\omega;\Theta)$ is any convex hull $\operatorname{conv}\{v_1(j\omega),v_2(j\omega),\ldots,v_n(j\omega)\}$ that contains $P(j\omega;\Theta)$:

$$P(j\omega;\Theta)\subset\operatorname{conv}\{v_1(j\omega),v_2(j\omega),\ldots,v_n(j\omega)\} \tag{23}$$

The following lemma and proposition are considered, which are important for the simplification of model approximation problem.

**Lemma 1.** The maximum distance from a fixed point $\tilde{v}$ in the complex plane to a convex hull $\operatorname{conv}\{v_1,v_2,\ldots,v_n\}$ is taken at one of the vertices $v_i\ (i=1,2,\ldots,n)$.

**Proof.** The reduction to absurdity method is utilized to prove this lemma. Suppose the maximum distance from $\operatorname{conv}\{v_1,v_2,\ldots,v_n\}$ to $v_0$ is taken at $\hat{v}$ that is not the vertex of the convex hull. Obviously, there exists a line segment in the convex hull that contains $\hat{v}$, and $\hat{v}$ is not the endpoint of the line segment:

$$\begin{aligned}&\hat{v}=\lambda\hat{v}_1+(1-\lambda)\hat{v}_2,0<\lambda<1\\&\hat{v}_1,\hat{v}_2\in\operatorname{conv}\{v_1,v_2,\ldots,v_n\}\end{aligned} \tag{24}$$

Therefore $|v_0-\hat{v}|<\max\left(|v_0-\hat{v}_1|,|v_0-\hat{v}_2|\right)$. This is in contradiction with the assumption that the maximum distance from the convex hull to $v_0$ is taken at $\hat{v}$ and thus ends the proof.

**Proposition 1.** Given a set of frequencies $\{\omega_1,\omega_2,\ldots,\omega_N\}$ and a series of convex hulls $\mathrm{conv}\{v_1(j\omega_k),v_2(j\omega_k),\ldots,v_n(j\omega_k)\}$ that contain the frequency template $P(s;\Theta)$ at frequency $\omega_k$ ($k=1,2,\ldots,N$), then an upper bound of the inner problem in (20) is given as:

$$\begin{aligned}\max_{\boldsymbol{\theta}\in\Theta}\left\|\boldsymbol{\Omega}-\boldsymbol{\Phi}(\boldsymbol{\theta})\cdot\boldsymbol{\beta}\right\|_2^2&=\max_{\boldsymbol{\theta}\in\Theta}\left\{\sum_{k=1}^{N}\left|T_r(j\omega_k)-p(j\omega_k;\boldsymbol{\theta})C(j\omega_k;\boldsymbol{\beta})\left(1-T_r(j\omega_k)\right)\right|^2\right\}\\&\le\sum_{k=1}^{N}\max_{i=1,2,\ldots,n}\left|T_r(j\omega_k)-v_i(j\omega_k)C(j\omega_k;\boldsymbol{\beta})\left(1-T_r(j\omega_k)\right)\right|^2\end{aligned}\tag{25}$$

**Proof.** Since $p(j\omega_k;\boldsymbol{\theta})\in\mathrm{conv}\{v_1(j\omega_k),v_2(j\omega_k),\ldots,v_n(j\omega_k)\}$, it is obvious that:

$$\begin{aligned}&p(j\omega_k;\boldsymbol{\theta})C(j\omega_k;\boldsymbol{\beta})\left(1-T_r(j\omega_k)\right)\in\\&\mathrm{conv}\left\{v_1(j\omega_k)C(j\omega_k;\boldsymbol{\beta})\left(1-T_r(j\omega_k)\right),\ldots,v_n(\omega_k j)C(j\omega_k;\boldsymbol{\beta})\left(1-T_r(j\omega_k)\right)\right\}\end{aligned}\tag{26}$$

Based on Lemma 1, the following inequality holds:

$$\begin{aligned}&\left|T_r(j\omega_k)-p(j\omega_k;\boldsymbol{\theta})C(j\omega_k;\boldsymbol{\beta})\left(1-T_r(j\omega_k)\right)\right|^2\le\\&\max_{i=1,2,\ldots,n}\left|T_r(j\omega_k)-v_i(j\omega_k)C(j\omega_k;\boldsymbol{\beta})\left(1-T_r(j\omega_k)\right)\right|^2,\ \forall\boldsymbol{\theta}\end{aligned}\tag{27}$$

Consequently

$$\begin{aligned}&\max_{\boldsymbol{\theta}\in\Theta}\left\{\sum_{k=1}^{N}\left|T_r(j\omega_k)-p(j\omega_k;\boldsymbol{\theta})C(j\omega_k;\boldsymbol{\beta})\left(1-T_r(j\omega_k)\right)\right|^2\right\}\\&\le\sum_{k=1}^{N}\max_{i=1,2,\ldots n}\left|T_r(j\omega_k)-v_i(j\omega_k)C(j\omega_k;\boldsymbol{\beta})\left(1-T_r(j\omega_k)\right)\right|^2\end{aligned}\tag{28}$$

That ends the proof.

Based on Proposition 1, the maximum approximation error at frequency $\omega_k$ is bounded by the worst case among the vertices of the convex hull that contains the frequency response template $P(\omega_k j;\Theta)$. Hence, instead of optimizing the time-consuming problem (20), one can minimize the worst approximation errors among the convex hull vertices to derive the desired PID parameters:

$$\begin{aligned}&\min_{\boldsymbol{\beta}} \bar{J}(\boldsymbol{\beta})\\&\bar{J}(\boldsymbol{\beta}) = \sum_{k=1}^{N} \max_{i=1,2,\ldots n} \left| T_r(j\omega_k) - v_i(j\omega_k) C(j\omega_k;\boldsymbol{\beta}) \right|^2\end{aligned} \tag{29}$$

This optimization problem is equivalent to the following constrained convex optimization problem:

$$\begin{aligned}&\min_{z_k \in \mathrm{R}, \boldsymbol{\beta} \in \mathrm{R}^3} \sum_{k=1}^{N} z_k^2\\&\text{s.t. } \left| T_r(j\omega_k) - v_i(j\omega_k) C(j\omega_k;\boldsymbol{\beta}) \right| \le z_k\\&i = 1, 2, \ldots, n\\&k = 1, 2, \ldots, N\end{aligned} \tag{30}$$

Hence the PID parameters can be searched in a cost efficient way by using elegant convex optimization procedures. Similar to the PID design for the single model case, in order to ensure the PID controller operate under proper frequencies, the upper bound $\omega_N$ of the frequency range is selected such that the minimal angle of the corresponding frequency template is $-\pi$:

$$\min\left\{ \mathrm{Arg}[p(j\omega_N)] \middle| p(j\omega_N) \in P(j\omega_N;\Theta) \right\} = -\pi \tag{31}$$

where $\mathrm{Arg}[p(j\omega_N)]$ is the angle of $p(j\omega_N)$.

### *4.2 Convex approximation of frequency templates*

For the optimization problem (30), it is necessary to establish an appropriate convex hull that can well approximate the frequency template $P(j\omega_k;\Theta)$. A natural approach is to first grid the whole parameter space or the edge of the parameters, and then establish the convex hull using the gridded frequency responses. Nevertheless, it must be emphasized that this approach may result in spurious computational burden since the number of the gridded frequency responses is increasing exponentially with the dimension of parameter space. In addition, most of the gridded frequency responses are internal points rather than the vertices

of the convex hull, and the computational burden for searching the vertices among the gridded frequency responses is another practice concern.

Alternatively, these practical issues can be handled by gridding the angle range of $P(j\omega;\Theta)$. First, for a given $\omega$, the angle range of $P(j\omega;\Theta)$, which is $\left[\phi^{-}(\omega),\phi^{+}(\omega)\right]$, would be estimated first. Then for a specified $\phi\in\left[\phi^{-}(\omega),\phi^{+}(\omega)\right]$, the minimal and maximum magnitudes of the frequency responses $p(j\omega;\boldsymbol{\theta})$ with the angle $\phi$ can be calculated by the following optimization problem:

$$\begin{aligned} & g^{+}(\phi,\omega)=\max\left|p(j\omega;\boldsymbol{\theta})\right| \\ & g^{-}(\phi,\omega)=\min\left|p(j\omega;\boldsymbol{\theta})\right| \\ & \text{s.t.} \\ & \boldsymbol{\theta}\in\Theta \\ & \operatorname{Arg}\left[p(j\omega;\boldsymbol{\theta})\right]=\phi \end{aligned} \tag{32}$$

Hence, the convex hull that approximates $P(j\omega;\Theta)$ is established as:

$$\operatorname{conv}\left\{g^{-}(\phi_1,\omega)e^{\phi_1 j},g^{+}(\phi_1,\omega)e^{\phi_1 j},\cdots,g^{-}(\phi_s,\omega)e^{\phi_s j},g^{+}(\phi_s,\omega)e^{\phi_s j}\right\} \tag{33}$$

where $\{\phi_1,\cdots,\phi_s\}$ are the gridded angles that are in the range $\left[\phi^{-}(\omega),\phi^{+}(\omega)\right]$. Since there is only one parameter required to be gridded, this approach needs much fewer gridded points. Nevertheless, it should be noted that the optimization problem (32) is non-linear programming (NLP) problem. In the following simple procedures are proposed to solve the NLP problem (32) in a cost efficient way.

The angle and magnitude of $p(j\omega;\boldsymbol{\theta})$ are calculated as follows:

$$\begin{aligned} &\operatorname{Arg}[p(\omega j;\boldsymbol{\theta})]=\operatorname{Arg}[\varphi_1(\boldsymbol{\theta},\omega)]+\operatorname{Arg}[\varphi_2(\boldsymbol{\theta},\omega)] \\ &\left|p(\omega j;\boldsymbol{\theta})\right|=K\left|\varphi_1(\boldsymbol{\theta},\omega)\right| \end{aligned} \tag{34}$$

where

$$\begin{aligned}\varphi_1(\boldsymbol{\theta},\omega)&=\frac{1}{\left(1-T_2^2\omega^2\right)+T_1\omega j},\\ \varphi_2(\boldsymbol{\theta},\omega)&=e^{-\tau\omega j}\end{aligned}\tag{35}$$

In addition, it should be noted that the set of $1/\varphi_1(\boldsymbol{\theta},\omega)$ is a rectangle in the complex plane since the model parameters $p(j\omega;\boldsymbol{\theta})$ are independent, which is denoted as $\Psi(\omega)$ as follows:

$$\Psi(\omega)=\left\{\frac{1}{\varphi_1(\boldsymbol{\theta},\omega)}\middle|\boldsymbol{\theta}\in\boldsymbol{\Theta}\right\}=\left\{x+yj\middle|\begin{array}{l}1-\left(T_2^+\omega\right)^2\le x\le 1-\left(T_2^-\omega\right)^2\\ T_1^-\omega\le y\le T_1^+\omega\end{array}\right\}\tag{36}$$

Because $\mathrm{Arg}[p(\omega j;\boldsymbol{\theta})]$ is the sum of $\mathrm{Arg}[\varphi_1(\boldsymbol{\theta},\omega)]$ and $\mathrm{Arg}[\varphi_2(\boldsymbol{\theta},\omega)]$, the ranges of $\mathrm{Arg}[p(\omega j;\boldsymbol{\theta})]$ can be calculated resorting to the ranges of $\mathrm{Arg}[\varphi_1(\boldsymbol{\theta},\omega)]$ and $\mathrm{Arg}[\varphi_2(\boldsymbol{\theta},\omega)]$. Given the model parameter range $\boldsymbol{\Theta}$, we arrive at the following proposition:

**Proposition 2.** Given the frequency $\omega$**,** for the model parameter range $\boldsymbol{\Theta}$ formulated in (3), the ranges of $\mathrm{Arg}[\varphi_1(\boldsymbol{\theta},\omega)]$ and $\mathrm{Arg}[\varphi_2(\boldsymbol{\theta},\omega)]$ are derived as:

$$a^-=\min\left(\mathrm{Arg}[\varphi_1(\boldsymbol{\theta},\omega)]\right)=\begin{cases}-\left(\arctan\dfrac{T_1^+\omega}{1-T_2^+\omega^2}\right),\omega<\dfrac{1}{\sqrt{T_2^+}}\\ -\left(\pi+\arctan\dfrac{T_1^-\omega}{1-T_2^+\omega^2}\right),\omega\ge\dfrac{1}{\sqrt{T_2^+}}\end{cases}\tag{37}$$

$$a^+=\max\left(\mathrm{Arg}[\varphi_1(\boldsymbol{\theta},\omega)]\right)=\begin{cases}-\left(\arctan\dfrac{T_1^-\omega}{1-T_2^-\omega^2}\right),\omega<\dfrac{1}{\sqrt{T_2^-}}\\ -\left(\pi+\arctan\dfrac{T_1^+\omega}{1-T_2^-\omega^2}\right),\omega\ge\dfrac{1}{\sqrt{T_2^-}}\end{cases}\tag{38}$$

$$b^-=\min\left(\mathrm{Arg}[\varphi_2(\boldsymbol{\theta})]\right)=-\tau^+\omega,\ b^+=\max\left(\mathrm{Arg}[\varphi_2(\boldsymbol{\theta})]\right)=-\tau^-\omega\tag{39}$$

**Proof.** The angles of $\mathrm{Arg}[\varphi_1]$ and $\mathrm{Arg}[\varphi_2]$ are derived as:

$$\begin{aligned}\text{Arg}[\varphi_1(\boldsymbol{\theta},\omega)] &= \begin{cases} -\left(\arctan\dfrac{T_1\omega}{1-T_2\omega^2}\right), \omega < \dfrac{1}{\sqrt{T_2}} \\ -\left(\pi+\arctan\dfrac{T_1\omega}{1-T_2\omega^2}\right), \omega \geq \dfrac{1}{\sqrt{T_2}} \end{cases} \\ \text{Arg}[\varphi_2(\boldsymbol{\theta},\omega)] &= -\tau\omega \end{aligned} \tag{40}$$

Once frequency $\omega$ is specified, it can be seen from (40) that $\text{Arg}[\varphi_2]$ is a decreasing function with respect to $\tau$. The function $f(T_1,T_2)=\arctan\dfrac{T_1\omega}{1-T_2\omega^2}$ is an increasing function with respect to $T_1$ and $T_2$ if $\omega<1/\sqrt{T_2}$, and it is a decreasing function with respect to $T_1$ and an increasing function with respect to $T_2$ if $\omega\geq 1/\sqrt{T_2}$. Hence Propositions 2 can be validated.

For a given $\text{Arg}\left[p(j\omega;\boldsymbol{\theta})\right]=\phi$, it implies that $\text{Arg}[\varphi_1(\boldsymbol{\theta},\omega)]+\text{Arg}[\varphi_2(\boldsymbol{\theta},\omega)]=\phi$ according to (34). Therefore, the range $\left[\phi^-(\omega),\phi^+(\omega)\right]$ of $\phi$ is:

$$\begin{aligned} &\text{Arg}[p(\omega j;\boldsymbol{\theta})]\geq\phi^-(\omega),\ \phi^-(\omega)=a^-+b^- \\ &\text{Arg}[p(\omega j;\boldsymbol{\theta})]\leq\phi^+(\omega),\ \phi^+(\omega)=a^++b^+ \end{aligned} \tag{41}$$

Once $\text{Arg}\left[p(j\omega;\boldsymbol{\theta})\right]$ is specified as $\phi$, the range of $\text{Arg}[\varphi_1(\boldsymbol{\theta},\omega)]$ will be constrained. The range of $\text{Arg}[\varphi_1(\boldsymbol{\theta},\omega)]$ under the constraint $\text{Arg}[\varphi_1(\boldsymbol{\theta},\omega)]+\text{Arg}[\varphi_2(\boldsymbol{\theta},\omega)]=\phi$ is denoted as $\left[c^-,c^+\right]$. Noticing that $\text{Arg}[\varphi_1(\boldsymbol{\theta},\omega)]$ and $\text{Arg}[\varphi_2(\boldsymbol{\theta},\omega)]$ are independent because the parameters of $p(j\omega;\boldsymbol{\theta})$ are independent as well, the constrained range $\left[c^-,c^+\right]$ of $\text{Arg}[\varphi_1(\boldsymbol{\theta},\omega)]$ with $\text{Arg}\left[p(j\omega;\boldsymbol{\theta})\right]$ being $\phi$ is calculated as follows:

$$\text{if } b^+-b^-<a^+-a^-,\ \left[c^-,c^+\right]=\begin{cases}\left[a^- \quad \phi-b^-\right],\ a^-+b^-\leq\phi<a^++b^- \\ \left[a^- \quad a^+\right],\ a^++b^-\leq\phi<a^-+b^+ \\ \left[\phi-b^+ \quad a^+\right],\ a^-+b^+\leq\phi\leq a^++b^+\end{cases} \tag{42}$$

$$\text{if } b^+-b^-\leq a^+-a^-,\ \left[c^-,c^+\right]=\begin{cases}\left[a^- \quad \phi-b^-\right],\ a^-+b^-\leq\phi<a^-+b^+ \\ \left[\phi-b^+ \quad \phi-b^-\right],\ a^-+b^+\leq\phi<a^++b^- \\ \left[\phi-b^+ \quad a^+\right],\ a^++b^-\leq\phi\leq a^++b^+\end{cases} \tag{43}$$

For a given $\mathrm{Arg}\left[p(j\omega;\boldsymbol{\theta})\right]=\phi$, the constrained range $\left[c^{-},c^{+}\right]$ of $\mathrm{Arg}[\varphi_1(\boldsymbol{\theta},\omega)]$ is calculated via (42) or (43). Noting the fact $\mathrm{Arg}[\varphi_1(\boldsymbol{\theta},\omega)]=-\mathrm{Arg}[1/\varphi_1(\boldsymbol{\theta},\omega)]$, the range of $\mathrm{Arg}[1/\varphi_1(\boldsymbol{\theta},\omega)]$ is also determined, which is $\left[-c^{+},-c^{-}\right]$. Because the magnitude of $p(j\omega;\boldsymbol{\theta})$ is only related with the $\varphi_1(\boldsymbol{\theta},\omega)$ and $K$, $g^{+}(\phi)$ and $g^{-}(\phi)$ of problem (32) can be calculated by the following problem:

$$\begin{aligned}
&q^{+}(\phi,\omega)=\max\left|x+yj\right|\\
&q^{-}(\phi,\omega)=\min\left|x+yj\right|\\
&\text{s.t.}\\
&1-\left(T_2^{+}\omega\right)^2\le x\le 1-\left(T_2^{-}\omega\right)^2\\
&T_1^{-}\omega\le y\le T_1^{+}\omega\\
&-c^{+}\le\mathrm{Arg}[x+yj]\le -c^{-}
\end{aligned}\tag{44}$$

Hence, $g^{+}(\phi,\omega)$ and $g^{-}(\phi,\omega)$ in (32) are computed as follows:

$$\begin{aligned}
g^{+}(\phi,\omega)&=\frac{K^{+}}{q^{-}(\phi,\omega)}\\
g^{-}(\phi,\omega)&=\frac{K^{-}}{q^{+}(\phi,\omega)}
\end{aligned}\tag{45}$$

The feasible region of the problem (44), which will be denoted as $\Gamma(\omega)$, is a convex polygon. An example of $\Gamma(\omega)$ is shown in Figure 2, and it is actually the remaining part of the rectangle $\Psi(\omega)$ in (36) cut by the lines $y=\tan\left(-c^{\pm}\right)x$. In addition, $\Gamma(\omega)$ is a convex hull expanded by its vertices, and it implies that both $q^{+}(\phi)$ and $q^{-}(\phi)$ can be calculated with ease noting that they are actually the maximum and minimal distance from the original point $(0,0)$ to $\Gamma(\omega)$, respectively.

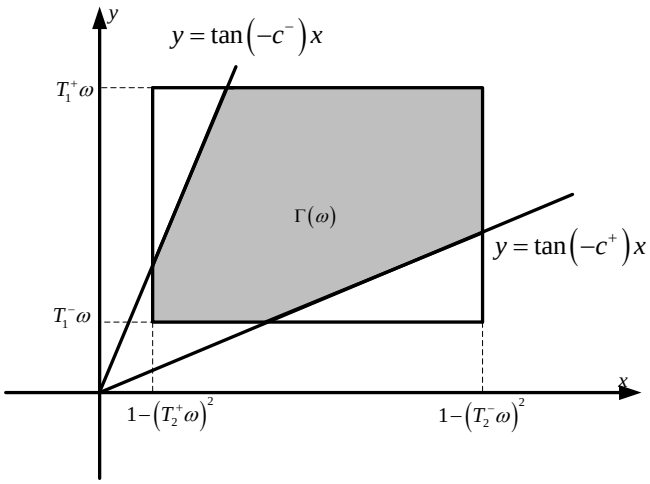


**Figure** 2 An example of $\Phi(\omega)$ showing the feasible region of problem (43)

**Proposition 3.** The maximum distance $q^+(\phi,\omega)$ from $(0,0)$ to $\Gamma(\omega)$ is achieved at the vertex of the $\Gamma(\omega)$.

**Proof.** Because $\Gamma(\omega)$ is the convex hull expanded by its vertices, Proposition 3 is the direct deduction of Lemma 1.

**Proposition 4.** If $\frac{\pi}{2}\notin\left[-c^+,-c^-\right]$**,** the minimum distance $q^-(\phi,\omega)$ from $(0,0)$ to $\Gamma(\omega)$ is achieved at the vertex of the $\Gamma(\omega)$.

**Proof.** The minimal distance is achieved at the edge of $\Gamma(\omega)$. Because $\frac{\pi}{2}\notin\left[-c^+,-c^-\right]$, it implies that $1-\left(T_2^+\omega\right)^2>0$ or $1-\left(T_2^-\omega\right)^2<0$. Hence all the edges are in the same quadrant, either in the first quadrant or the second quadrant. For the edges that are parallel to the *x*-axis or *y*-axis, the minimal distance to $(0,0)$ is achieved at their endpoints because the edges are in the same quadrant. For the edges that are in the line $y=\tan\left(-c^+\right)x$ or $y=\tan\left(-c^-\right)x$, the minimal distance to $(0,0)$ is at the endpoints as well noting that $(0,0)$ is also in the lines $y=\tan\left(-c^\pm\right)x$. Because the endpoints of the edges are also the vertices of $\Gamma(\omega)$, Proposition 4 can be validated.

**Proposition 5.** If $\frac{\pi}{2} \in \left[-c^+, -c^-\right]$, the minimum distance $q^-(\phi)$ from the origin $(0,0)$ to $\Gamma(\omega)$ is achieved at the point $\left(0, T_1^- \omega\right)$.

**Proof.** If $\frac{\pi}{2} \in \left[-c^+, -c^-\right]$, it implies that $1-\left(T_2^+ \omega\right)^2 \le 0$ and $1-\left(T_2^- \omega\right)^2 \ge 0$. Note that $\left(0, T_1^- \omega\right) \in \Gamma(\omega)$ and $T_1^- \omega > 0$, Proposition 5 can be easily validated and the proof is omitted for brevity.

Resorting to Propositions 3-5, solving the problem (32) is equivalent to finding the vertices of $\Phi(\omega)$, which can be accomplished in a cost efficient way. The following algorithm is proposed to calculate the convex hull that approximates $P(j\omega;\Theta)$:

Step 1. Calculate the angle ranges $\left[\phi^-(\omega), \phi^+(\omega)\right]$ of $p(j\omega;\theta)$ using Equations (37)-(39) and (41).

Step 2. Partition the range $\left[\phi^-(\omega), \phi^+(\omega)\right]$ into *s* grids $\phi_1$, $\phi_2$, … , $\phi_s$ with $\phi^-(\omega) = \phi_1$ and $\phi^+(\omega) = \phi_s$.

Step 3. Set *i*=1.

Step 4. Calculate the constrained angle range $\left[c^-, c^+\right]$ of $\varphi_1(\theta, \omega)$ under the constraint $\text{Arg}[\varphi_1(\theta, \omega)] + \text{Arg}[\varphi_2(\theta, \omega)] = \phi_i$ using (42) and (43).

Step 5. Calculate the vertices of $\Gamma(\omega)$.

Step 6. Calculate $q^+(\phi_i, \omega_k)$ and $q^-(\phi_i, \omega)$ using Propositions 3-5, and calculate $g^+(\phi_i, \omega)$ and $g^-(\phi_i, \omega)$ using (45).

Step 7. Increment *i*=*i*+1 and repeat Steps 4-5 until *i*=*s*.

Step 8. Establish the convex hull that approximates $P(j\omega;\Theta)$ as $\text{conv}\left\{g^-(\phi_1, \omega)e^{\phi_1 j}, g^+(\phi_1, \omega)e^{\phi_1 j}, \cdots, g^-(\phi_s, \omega)e^{\phi_s j}, g^+(\phi_s, \omega)e^{\phi_s j}\right\}$.

***4.3 Convex-concave procedure for constraints on loop robustness***

Pursuing optimal control performance regardless of loop robustness is not advisable in industrial applications, and practical constraints on loop robustness should be considered to guarantee reasonable tuning. The robustness is quantified in terms of the sensitivity peak $M_S$:

$$M_S\left(P(s),C(s)\right)=\max_{\omega}\left|\frac{1}{1+P(j\omega)C(j\omega)}\right| \tag{46}$$

The index $M_S$ is actually the inverse of minimal distance of point (-1, 0) in the complex plane to the Nyquist plot of $P(j\omega)C(j\omega)$, and lower values of $M_S$ indicates improved robustness. A practical approach is to impose constraints on the following 8 cases $p_l(s)$ ($l=1,2,\cdots,8$) with the most extreme dynamics to guarantee loop robustness:

$$\begin{aligned}
p_1(s)&=\frac{K^+}{T_2^+s^2+T_1^+s+1}e^{-\tau^+s},\ p_2(s)=\frac{K^+}{T_2^-s^2+T_1^+s+1}e^{-\tau^+s}\\
p_3(s)&=\frac{K^+}{T_2^+s^2+T_1^-s+1}e^{-\tau^+s},\ p_4(s)=\frac{K^+}{T_2^-s^2+T_1^-s+1}e^{-\tau^+s}\\
p_5(s)&=\frac{K^-}{T_2^+s^2+T_1^+s+1}e^{-\tau^+s},\ p_7(s)=\frac{K^-}{T_2^-s^2+T_1^+s+1}e^{-\tau^+s}\\
p_6(s)&=\frac{K^-}{T_2^+s^2+T_1^-s+1}e^{-\tau^+s},\ p_8(s)=\frac{K^-}{T_2^-s^2+T_1^-s+1}e^{-\tau^+s}
\end{aligned} \tag{47}$$

A larger process delay is not beneficial for loop stability and reduces the phase margin, and hence the constraints on the maximum sensitivity are imposed on the models with the largest process delay. The gains and time constants of $p_l(s)$ are either the minimal or the maximum values of the corresponding parameter range, and these models have the most extreme dynamic properties, including the most intense or insensive response for controller actions. Hence unreasonable tuning with low robustness degree is avoided by considering the additional constraints on $M_S$ of these extreme cases:

$$\left|\frac{1}{1+p_l(\tilde{\omega}_n j)C(\tilde{\omega}_n j;\boldsymbol{\beta})}\right| \le \delta_S$$
$$l=1,\ldots,8$$
$$n=1,2,\ldots,M \tag{48}$$

where $\delta_S$ is the specified maximum allowable sensitive peak value for these extreme cases, and $\tilde{\omega}_n$ $(1 \le n \le M)$ are the gridded frequencies for estimation of the sensitive peak. The range of $\tilde{\omega}_n$ should be wide enough to cover the dominant frequency range of the sensitivity function. Constraints (48) are equivalent to the following circle constraints:

$$\frac{1}{\delta_S} - \left|1+p_l(\tilde{\omega}_n j)C(\tilde{\omega}_n j;\boldsymbol{\beta})\right| \le 0 \tag{49}$$

The reference model approximation problem with constraints on loop robustness is formulated as follows:

$$\begin{aligned}
&\min_{z_k \in \mathrm{R}, \boldsymbol{\beta} \in \mathrm{R}^3} \sum_{k=1}^{N} z_k^2 \\
&\text{s.t.} \\
&\left|T_r(j\omega_k) - v_i(j\omega_k)C(j\omega_k;\boldsymbol{\beta})\right| \le z_k, \ \forall i,k \\
&\frac{1}{\delta_S} - \left|1+p_l(\tilde{\omega}_n j)C(\tilde{\omega}_n j;\boldsymbol{\beta})\right| \le 0 \ , \ \forall l,n
\end{aligned} \tag{50}$$

The constraints (49) are not convex, and hence convex optimization technique cannot be applied to (50) directly. Nevertheless, constraints (49) are the difference of two convex functions, which can be relaxed as convex constraints using the standard convex-concave programming (CCP):[27-29]

$$\frac{1}{\delta_S} - \mathrm{Re}\left( \frac{\left(1+p_l(\tilde{\omega}_n j)C(\tilde{\omega}_n j;\boldsymbol{\beta}_q)\right)^*}{\left|1+p_l(\tilde{\omega}_n j)C(\tilde{\omega}_n j;\boldsymbol{\beta}_q)\right|} \left(1+p_l(\tilde{\omega}_n j)C(\tilde{\omega}_n j;\boldsymbol{\beta})\right) \right) \le 0 \tag{51}$$

where "*" denotes the complex conjugate and $\boldsymbol{\beta}_q = (K_p^q, K_i^q, K_d^q)^T$ is a known feasible PID solution that satisfies the constraints (49). The detailed principle of CCP and derivation of (51)

is reviewed in the Appendix. The constraints (51) are actually linear inequalities and are thus convex. By replacing constraints (49) by their convex-concave relaxations, a relaxed convex problem can be derived:

$$\begin{aligned}
&\min_{z_k\in\mathrm{R},\boldsymbol{\beta}\in\mathrm{R}^3}\sum_{k=1}^{N}z_k^2\\
&\text{s.t.}\\
&\left|T_r\left(j\omega_k\right)-v_i\left(j\omega_k\right)C\left(j\omega_k;\boldsymbol{\beta}\right)\right|\le z_k,\forall i,k\\
&\frac{1}{\delta_S}-\mathrm{Re}\left(\frac{\left(1+p_l\left(\tilde{\omega}_n j\right)C\left(\tilde{\omega}_n j;\boldsymbol{\beta}_q\right)\right)^*}{\left|1+p_l\left(\tilde{\omega}_n j\right)C\left(\tilde{\omega}_n j;\boldsymbol{\beta}_q\right)\right|}\left(1+p_l\left(\tilde{\omega}_n j\right)C\left(\tilde{\omega}_n j;\boldsymbol{\beta}\right)\right)\right)\le 0,\forall l,n
\end{aligned}\tag{52}$$

It should be noted that the constraints (51) are stricter than the original constraints, which means that the PID parameter vector $\boldsymbol{\beta}$ guarantees to satisfy the constraints (49) if constraints (51) are also satisfied. Hence, the feasible set of the relaxed problem (52) is a convex subset of the problem (50). To approximate the optimal solution to the original problem (50), an iterative procedure is applied in the convex-concave optimization framework. Denote the optimal PID parameters of the $q$'th iteration to problem (52) as $\boldsymbol{\beta}_q$, and it can be used to generate the optimization problem as (52) for the ($q$+1)'th iteration. The optimal solution $\boldsymbol{\beta}_{q+1}$ to the ($q$+1)'th iteration is guaranteed to be feasible, because the relaxed constraints are stricter and the original constraints can be satisfied. Meanwhile, the optimal objective value of $\boldsymbol{\beta}_{q+1}$ is not increased compared to the last iteration, and finally the iterated optimal objective would converge to a saddle point or a local minimum.[29] Even though it is not guaranteed that a global solution can be searched, the convex-concave procedures can usually provide satisfactory solutions.[29] The detailed optimization procedure is depicted as follows.

Step 1. Grid the frequency as $\{\omega_k\}$ and $\{\tilde{\omega}_n\}$. The maximum frequency $\omega_N$ of the gridded

frequency $\{\omega_k\}$ should satisfy $\min\left\{\text{Arg}[p(j\omega_N)]\middle| p(s)\in P(j\omega_N;\Theta)\right\}=-\pi$, while $\{\tilde{\omega}_n\}$ should cover the dominant frequency range of the closed-loop system.

Step 2. For each gridded frequency $\omega_k$ in $\{\omega_k\}$, establish the convex hull $\text{conv}\left\{g^-(\phi_1,\omega_k)e^{\phi_1 j}, g^+(\phi_1,\omega_k)e^{\phi_1 j},\cdots, g^-(\phi_s,\omega_k)e^{\phi_s j}, g^+(\phi_s,\omega_k)e^{\phi_s j}\right\}$ of $P(j\omega_k;\Theta)$ using the method proposed in Section 4.2, and the set $\{v_i(j\omega_k)\}$ in problem (50) is specified as $\left\{g^-(\phi_1,\omega_k)e^{\phi_1 j}, g^+(\phi_1,\omega_k)e^{\phi_1 j},\cdots, g^-(\phi_s,\omega_k)e^{\phi_s j}, g^+(\phi_s,\omega_k)e^{\phi_s j}\right\}$.

Step 3. Find an initial solution $\beta_0$ to the problem (50). A proper initialization can be a very conservative PID with a small gain, small derivative time and long integral time.

Step 4. Set $q$=1.

Step 5. Relax the constraints via (51) using the optimal solution $\beta_{q-1}$ obtained from the last iteration, and search the optimal solution $\beta_q$ to the relaxed convex problem (52) using convex optimization techniques.

Step 6. If $\left|f(\beta_q)-f(\beta_{q-1})\right|\le\varepsilon$ where $f(\beta_q)$ denotes the optimal objective of the $q$'th iteration and $\varepsilon$ is the prespecified tolerance, then stop the iterative procedure and export the optimized PID parameter $\beta_q$. Otherwise increase $q$=$q$+1 and return to Step 5 to continue the convex-concave procedure.

# 5. CASE STUDIES

### *5.1 An illustrative example*

In this section, a numerical example is presented to demonstrate the applicability of the proposed method. The purpose of this section is to show that the reference model shaping considerations can be incorporated into the design procedure such that the different tuning objective can be achieved.

Consider the following parametric uncertain process:

$$P(s;\Theta)=\left\{\frac{K}{T_2 s^2+T_1 s+1}e^{-\tau s}\right\}$$
$$0.7\le K\le 1.3, 10\le \tau\le 20, \quad (53)$$
$$60\le T_1\le 110, 525\le T_2\le 975$$

Achieving satisfactory tracking performance is a very common PID design objective in practice, and hence the following reference model is adopted for PID design:

$$T_r^1(s)=\frac{1}{14.38^2 s^2+1.6\cdot 14.38 s+1}e^{-20s} \quad (54)$$

This damping ratio of the reference model is 0.8 to yield a smooth setpoint response. The delay of $T_r(s)$ is set to be equal to the maximum delay. The response speed is restricted by the process delay, and $\lambda$ is chosen to be 14.38 such that the time constant of $T_r(s)$ would not be much shorter than the delay of the controlled process and the resulting closed-loop response would be reasonable. To guarantee loop robustness, $\delta_S$ in optimization problem (50) is restricted not to exceed 2, and the resulting PID controller is $C_1(s)=1.52\left(1+\frac{1}{63.6s}+12.4s\right)$. Even though the constraints are only imposed on the 8 extreme cases, the resulting worst-case sensitivity peak of $P(s;\Theta)$ is 2. The step response of $C_1(s)$ with respect to the parameter uncertain process $P(s;\Theta)$ is shown in Figure 4, and each trajectory represents the closed-loop set-point response for a possible candidate model. It can be seen that the step response of each candidate model of $P(s;\Theta)$ is smooth, and thus the tracking performance can be quantified to be satisfactory.

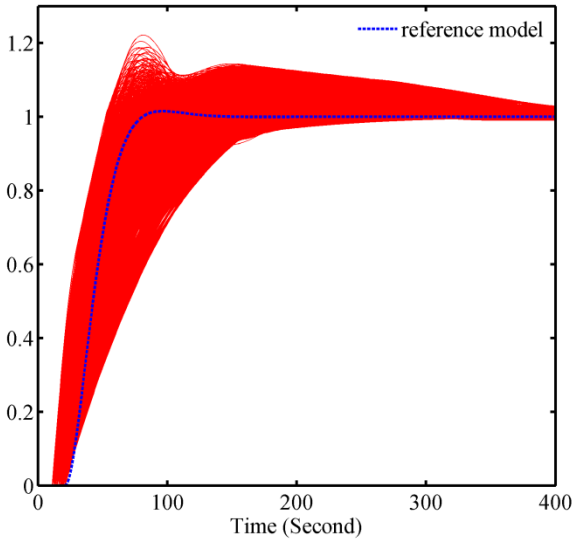


**Figure** 4 Step responses of $C_1(s)$ subject to setpoint changes with respect to $P(s;\Theta)$

In general, the servo performance and regulatory performance can hardly be guaranteed simultaneously by 1DOF PID controllers. Hence the sluggish response to the input disturbance is the side effect of a smooth setpoint response. To compensate this issue, the following reference model with a lead part is adopted with the purpose for improving the disturbance rejection performance:

$$T_r^2(s)=\frac{1.5*34.38s+1}{34.38^2s^2+1.6\cdot 34.38s+1}e^{-20s} \tag{55}$$

To ensure similar robustness degree as $C_1(s)$, $\delta_S$ in optimization problem (50) is restricted not to exceed 2, and the worst-case sensitivity peak is 2 as well. The resulting PID controller is $C_2(s)=1.54\left(1+\frac{1}{35.9s}+17.4s\right)$. The step response of $C_2(s)$ and the reference model $T_r^2(s)$ subject to the setpoint change is shown in Figure 5. Compared to $C_1(s)$, the PID controller $C_2(s)$ designed using the reference model $T_r^2(s)$ for improved disturbance rejection performance would yield smaller integral time and the overshoots are larger. The response of $C_1(s)$ and $C_2(s)$ subject to step input load disturbance for $P(s;\Theta)$ is compared in Figure 6, and it can be observed that the settling time of $C_2(s)$ is shorter than

that of $C_1(s)$ in general, and the hence $C_2(s)$ have improved disturbance rejection performance compared to $C_1(s)$. To quantify the tracking performance and disturbance rejection performance, the average IAE values for step setpoint changes and input load disturbances, which are calculated by gridding the parameter ranges of $P(s;\Theta)$, are compared in Table 1. At the expenses of increasing the overshoot of the setpoint response, it is concluded that the disturbance rejection performance can be improved significantly. Even though a 1DOF PID controller can hardly ensure improved set-point tracking performance and load disturbance rejection performance simultaneously, it can be seen from this example that the proposed method still provides a flexible approach to PID design for different tuning objectives. The reference model approach can guarantee either improved tracking performance or disturbance rejection performance by specifying different types of reference models, depending on the practical control objective.

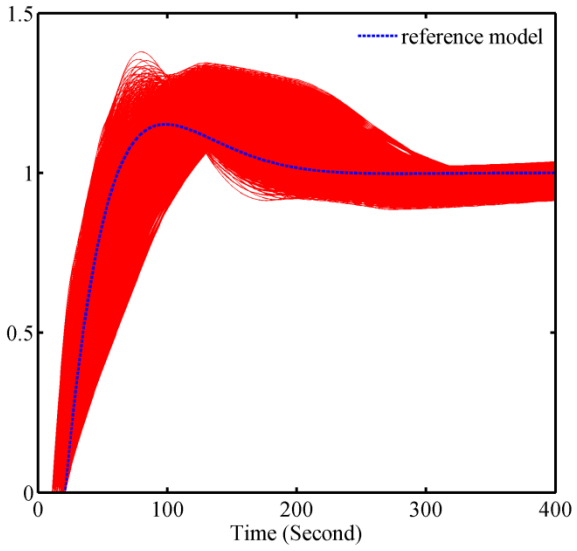


**Figure** 5 Step responses of $C_2(s)$ subject to setpoint changes with respect to $P(s;\Theta)$

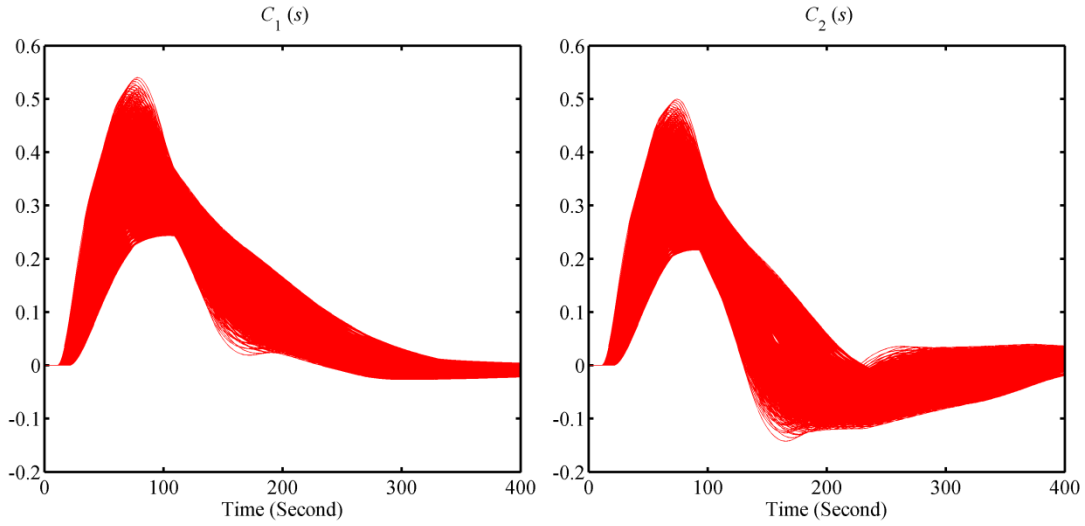


**Figure** 6 Step responses of $C_1(s)$ and $C_2(s)$ subject to input load disturbance with respect to $P(s;\Theta)$

**Table 1** Average IAE of $C_1(s)$ and $C_2(s)$ with respect to $P(s;\Theta)$

| PID | Average IAE | |
|---|---|---|
| | Setpoint tracking | Disturbance rejection |
| $C_1(s)$ | 57.5 | 43.8 |
| $C_2(s)$ | 66.3 | 36.2 |

### *5.2 Evaluation of the proposed method*

In this section, the effectiveness of the proposed method is validated through representative numerical examples. In order to cover a wider range of process dynamics, this section would consider one lag-dominant process, one with balanced lag and delay and one delay-dominant process:

$$\begin{aligned} p_1(s) &= \frac{1}{1000s^2+110s+1}e^{-10s} \\ p_2(s) &= \frac{1}{400s^2+50s+1}e^{-40s} \\ p_3(s) &= \frac{1}{20s^2+12s+1}e^{-50s} \end{aligned} \tag{56}$$

The processes $P_1(s;\Theta)\sim P_3(s;\Theta)$ with parametric uncertainty are extended by the nominal models $p_1(s)\sim p_3(s)$ as the center respectively, and each parameter has an uncertainty of $\pm 30\%$. For comparison purposes, the SIMC and AMIGO tuning rules are studied because

these two existing approaches can be complemented with ease and provide effective tuning in most scenarios. The SMIC tuning and AMIGO tuning are based on the nominal models $p_1(s)$ ~ $p_3(s)$. Even though these two design methods are aimed at a single linear model, loop robustness for model uncertainties can still be guaranteed by applying a reasonable tuning. To achieve a balance between tracking performance and disturbance rejection performance, the following reference model was utilized by the proposed method:

$$T_r(s) = \frac{0.8\lambda s + 1}{\lambda^2 s^2 + 1.6\lambda s + 1} e^{-\tau s} \tag{57}$$

For all the PID design methods, the $M_S$ for the worst case among all the candidate models are specified to be the same such that a similar robustness degree for different design methods is ensured.

The average IAE values subject to step setpoint changes and input load disturbance are utilized to quantify the set-point tracking and disturbance rejection performance, which are calculated by gridding the parameters of $P_1(s;\Theta) \sim P_3(s;\Theta)$, In Table 1, related performance measures are listed, and the closed-loop responses of different PID design methods for the step set-point change and load disturbance are shown in Figures 7~9. For almost all cases, the proposed method can achieve both improved tracking performance and disturbance rejection performance compared to the SIMC PID and AMIGO PID, except for the lag-dominant process $P_1(s;\Theta)$ where the tracking performance of SIMC PID is comparable to that of the proposed method. Yet in this case the disturbance rejection performance of the proposed PID is much better than that of the SIMC, which means that the tuning parameters by the proposed method are more reasonable. Furthermore, a feature of the proposed method is that it can be applied to a wider range of process dynamics. As indicated in Table 2, the SIMC PID would

yield poor tuning for the delay-dominant process $P_3(s;\Theta)$, while the parameters of AMIGO PID are conservative for the lag-dominant process $P_1(s;\Theta)$. In contrast, the proposed method can guarantee satisfactory performance for all the cases $P_1(s;\Theta)\sim P_3(s;\Theta)$ in spite of the divergent dynamic properties.

**Table 2.** Performance assessment of different PID tuning methods

| process | Design methods | PID parameters $K_p$ | $T_i$ | $T_d$ | Average IAE Setpoint | Disturbance | worst-case $M_s$ |
|---|---|---|---|---|---|---|---|
| $P_1(s;\Theta)$ | Proposed PID | 2.80 | 63.1 | 12.0 | 45.4 | 24.1 | 1.85 |
| | SIMC-PID | 2.70 | 100 | 10 | 45.3 | 37.1 | 1.85 |
| | AMIGO-PID | 2.05 | 72.5 | 7.15 | 55.8 | 36.3 | 1.85 |
| $P_2(s;\Theta)$ | Proposed PID | 0.483 | 38.1 | 24.3 | 106.4 | 96.7 | 1.94 |
| | SIMC-PID | 0.359 | 40.00 | 10.00 | 126.2 | 118.74 | 1.94 |
| | AMIGO-PID | 0.465 | 53.74 | 14.65 | 123.2 | 117.1 | 1.94 |
| $P_3(s;\Theta)$ | Proposed PID | 0.262 | 26.5 | 11.7 | 108.1 | 104.0 | 1.92 |
| | SIMC-PID | 0.0745 | 10 | 2 | 144.3 | 138.82 | 1.92 |
| | AMIGO-PID | 0.261 | 27.29 | 9.46 | 111.2 | 106.5 | 1.92 |

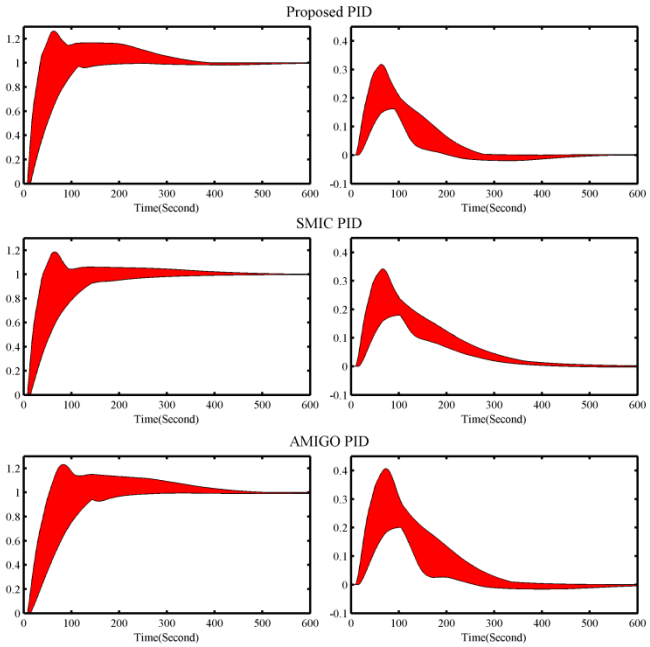


**Figure** 7 Closed-loop responses of different PID methods for $P_1(s)$

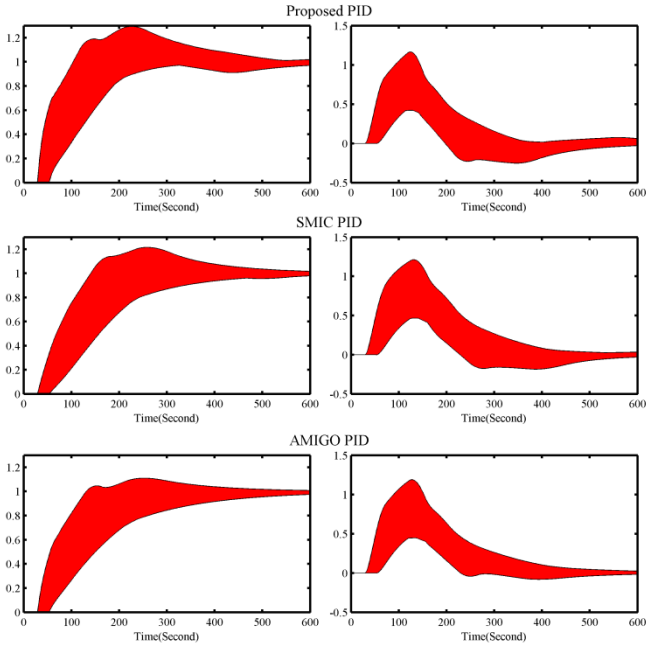


**Figure** 8 Closed-loop responses of different PID methods for $P_2(s)$

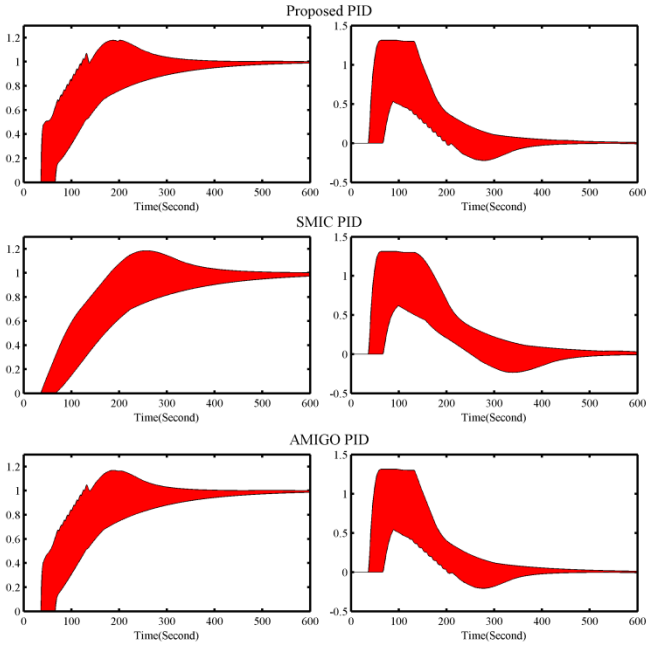


**Figure** 9 Closed-loop responses of different PID methods for $P_3(s)$

### *5.3 Validation on a nonlinear process*

In this section, the effectiveness of the proposed method is validated through a nonlinear process. It is the furnace control system for preheating the crude oil in a refinery plant, and a

brief sketch of this unit is shown in Figure 10. The fuel and air is mixed and burnt in the furnace to preheat the crude oil. The outlet temperature is controlled by a PID controller with the fuel flow as the manipulated variable. Through mechanism analysis, the fuel flow has the dominant influence on the outlet temperature, and the process dynamics can be well approximated by SOPTD models. This unit is simulated on the widely applied process simulation software in the process industry, which is Honeywell UniSim Design R410.

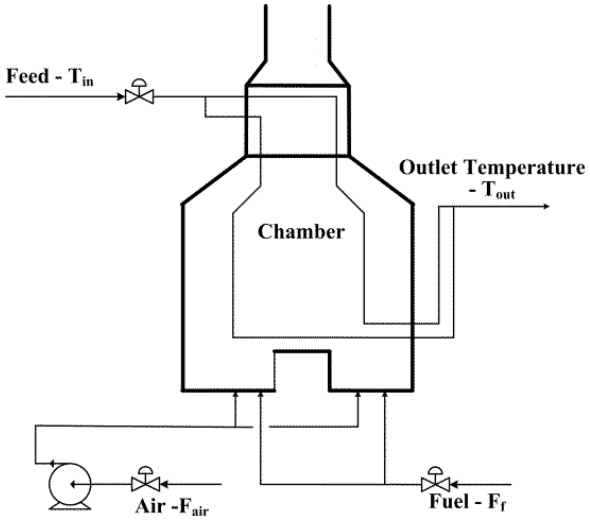


**Figure 10.** The sketch of the furnace

The controlled processes have significant nonlinear dynamics, which implies that locally linearized models obtained at different operating conditions have significant divergence with each other. Especially, the inlet feed flow has the most prominent influences on the process dynamics because the thermal load is closely related with the feed flow. Consider the operating point of the feed flow in the range of [150, 200] ton/h. Data-driven identification methods were applied for process modeling. To design a proper PID controller for this nonlinear process, 3 different linearized models were identified using closed-loop operating data from 3 different operating points:

$$\begin{aligned}
&\text{Feed folw=150 ton/h: } p_1(s) = \frac{0.79}{3607s^2 + 265.4s + 1} e^{-4s} \\
&\text{Feed folw=175 ton/h: } p_2(s) = \frac{0.59}{2713s^2 + 247.7s + 1} e^{-4s} \\
&\text{Feed folw=200 ton/h: } p_3(s) = \frac{0.45}{2096s^2 + 219.8s + 1} e^{-4s}
\end{aligned} \tag{58}$$

Hence, the following parametric uncertain SOPTD model $P(s;\Theta)$ was used by the proposed method, which are obtained by combinations of the linearized models $p_1(s) \sim p_3(s)$

$$P(s;\Theta) = \left\{ \frac{K}{T_2 s^2 + T_1 s + 1} e^{-\tau s} \middle| \begin{matrix} 0.44 \le K \le 0.8, 210 \le T_1 \le 270 \\ 2050 \le T_2 \le 3650, \tau = 4 \end{matrix} \right\} \tag{59}$$

The following reference model was used by the proposed method for a balanced tracking and disturbance rejection performance.

$$T_r(s) = \frac{8.8s + 1}{64s^2 + 12.8s + 1} e^{-4s} \tag{60}$$

The SIMC PID was tuned based on the nominal model:

$$p_0(s) = \frac{0.62}{2850s^2 + 240s + 1} e^{-4s} \tag{61}$$

The Amigo PID was tuned based on the first-order approximation $\tilde{p}_0(s)$ of $p_0(s)$:

$$\tilde{p}_0(s) = \frac{0.62}{230s + 1} e^{-14s} \tag{62}$$

For all the PID design methods, the PID parameters are tuned to ensure that the worst-case sensitivity peak $M_S$ among all candidate models in $P(s;\Theta)$ is 1.62. To evaluate the set-point tracking performance and disturbance rejection performance, step changes are introduced to the outlet temperature set point and the feed flow set point respectively.

The PID parameters and the corresponding closed-loop performance under the 3 different operating conditions of different methods are listed in Table 3, and Figure 10 shows the closed-loop responses for the step setpoint change and input load disturbance. The proposed PID can achieve reasonable set-point tracking performance and disturbance

rejection performance under the 3 different operating conditions. The tracking performance is satisfactory with the lowest ISE among all the methods, and meanwhile the overshoots are acceptable as well, which do not exceed 15%. Moreover, the load disturbance rejection performance of the proposed PID is much better than the other two PID controllers because both the corresponding ISE and the settling time are the lowest, as shown in Figure 10. For the SIMC PID, the set-point tracking performance is quantified to be good due to the smooth response and the reasonable ISE. Nevertheless, the disturbance rejection performance is poor and it takes a long time for the SIMC PID to eliminate the control error, and this is the side effect of SIMC tuning. This process is a typical lag-dominant process that has a much larger process time constant than the delay, and hence the AMIGO PID would yield an improper tuning with an overly small controller gain and integral time in this case. It is concluded that the proposed method is more reasonable because of a balanced set-point tracking and disturbance rejection performance.

**Table 3.** Performance assessment of different PID tuning methods

| Feed flow | Design methods | PID parameters | | | IAE | |
|---|---|---|---|---|---|---|
| | | $K_p$ | $T_i$ | $T_d$ | Setpoint | Disturbance |
| 150 | Proposed PID | 38.2 | 188 | 7.34 | 80.2 | 83.3 |
| | SIMC-PID | 28.1 | 228 | 12.4 | 85.2 | 136.3 |
| | AMIGO-PID | 14.9 | 72.8 | 5.37 | 92.4 | 120.7 |
| 175 | Proposed PID | | | | 82.9 | 97.7 |
| | SIMC-PID | | | | 86.7 | 159.6 |
| | AMIGO-PID | | | | 95.2 | 131.3 |
| 200 | Proposed PID | | | | 84.3 | 115.3 |
| | SIMC-PID | | | | 87.1 | 188.0 |
| | AMIGO-PID | | | | 96.4 | 144.6 |

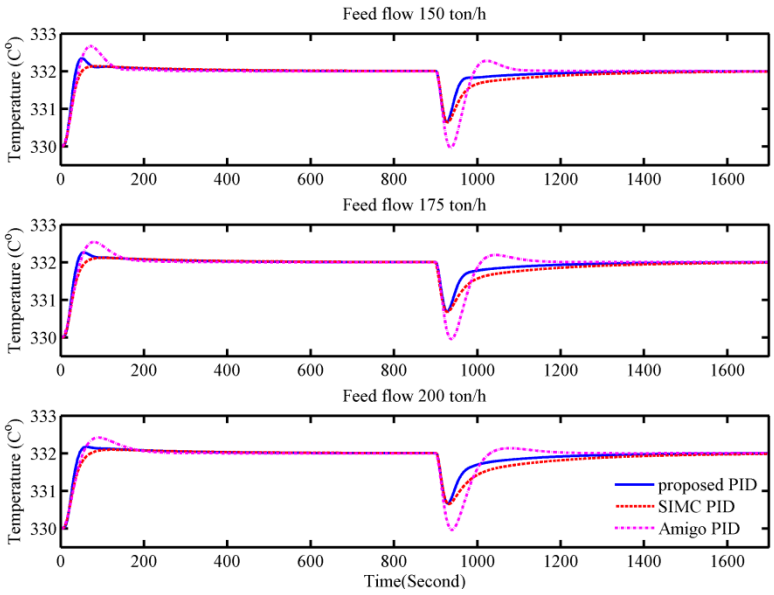


**Figure 10.** Closed-loop responses of different PID controllers

## 6. CONCLUSIONS

In this article, a reference-model approximation PID design method for parameter uncertain SOPTD processes is proposed. The presented method relies on approximating the frequency responses of a user-specified reference model such that the closed-loop set-point trajectory can approach to that of the reference model. Resorting to the convex hull that approximates the frequency template of the SOPTD process with model uncertainty, a convex optimization problem is formulated to derive expected PID parameters. Constraints on the maximum sensitive peak are added to guarantee the loop robustness, which are further relaxed as linear inequality constraints based on the standard convex-concave procedures to preserve the computation efficiency. By a proper design of the reference model, the proposed design method can guarantee balanced tracking performance and disturbance rejection performance.

## APPENDIX: THE CONVEX-CONCAVE PROGRAMMING (CCP)

The convex-concave programming is an effective procedure to relax inequality constraints that are formulated as a difference between two convex functions:[29]

$$f_i(\boldsymbol{\beta}) - g_i(\boldsymbol{\beta}) \le 0 \quad i = 1, ..., m \tag{A1}$$

where $f_i(\boldsymbol{\beta})$ and $g_i(\boldsymbol{\beta})$ are convex functions. The feasible region $\{\boldsymbol{\beta}\}$ of (A1) is non-convex because $-g_i(\boldsymbol{\beta})$ is nonconvex. The affine approximation of $g_i(\boldsymbol{\beta})$ at $\boldsymbol{\beta}_q$ is:

$$\hat{g}_i(\boldsymbol{\beta}; \boldsymbol{\beta}_q) = g_i(\boldsymbol{\beta}_q) + \nabla g_i(\boldsymbol{\beta}_q)^T (\boldsymbol{\beta} - \boldsymbol{\beta}_q) \tag{A2}$$

where $\nabla g_i(\boldsymbol{\beta}_q)$ is the gradient of $g_i(\boldsymbol{\beta})$ at $\boldsymbol{\beta}_q$. By replacing $g_i(\boldsymbol{\beta})$ by their affine approximations, (A1) can be relaxed as:

$$f_i(\boldsymbol{\beta}) - \hat{g}_i(\boldsymbol{\beta}; \boldsymbol{\beta}_q) \le 0 \quad i = 1, ..., m \tag{A3}$$

The constraints (A3) are convex. Because $g_i(\boldsymbol{\beta})$ is convex, it is obvious that $\hat{g}_i(\boldsymbol{\beta}; \boldsymbol{\beta}_q) \le g_i(\boldsymbol{\beta})$, and hence $f_i(\boldsymbol{\beta}) - g_i(\boldsymbol{\beta}) \le f_i(\boldsymbol{\beta}) - \hat{g}_i(\boldsymbol{\beta}; \boldsymbol{\beta}_q)$. Hence, constraints (A1) are guaranteed if (A3) is fulfilled, and the feasible region of (A3) is the convex subset of (A1).

Using CCP, constraints (49) can be relaxed as (51) noting the fact the affine approximation of $\left|1 + p_l(\tilde{\omega}_n j) C(\tilde{\omega}_n j; \boldsymbol{\beta})\right|$ at $\boldsymbol{\beta}_q$ is : [27, 28]

$$\mathrm{Re}\left( \frac{\left(1 + p_l(\tilde{\omega}_n j) C(\tilde{\omega}_n j; \boldsymbol{\beta}_q)\right)^*}{\left|1 + p_l(\tilde{\omega}_n j) C(\tilde{\omega}_n j; \boldsymbol{\beta}_q)\right|} \left(1 + p_l(\tilde{\omega}_n j) C(\tilde{\omega}_n j; \boldsymbol{\beta})\right) \right) \le 0 \tag{A4}$$

**Acknowledgments**

This work is supported in part by the National Natural Science Foundation of China (61433001 and 61673236), the National Basic Research Program of China (2012CB720505), the seventh framework programme of the European Union (P7-PEOPLE-2013-IRSES-612230), and Tsinghua University Initiative Scientific Research Program.

## REFERENCES

1. Desborough, L.; Miller, R. Increasing customer value of industrial control performance monitoring-Honeywell's experience. *AIChE Symposium Series;* American Institute of Chemical Engineers: 2002; pp 169-189.

2. Hang, C. C.; Astrom, K. J.; Ho, W. K. Refinements of the Ziegler-Nichols tuning formula. *IEE Proceedings*

*D-Control Theory and Applications;* IET: 1991; pp 111-118.

3. Åström, K.; Hägglund, T. Revisiting the Ziegler–Nichols step response method for PID control. *J. Process Control* **2004,** *14*, 635-650.

4. Rivera, D. E.; Morari, M.; Skogestad, S. Internal model control: PID controller design. *Ind. Eng. Chem. Process Des. Dev.* **1986,** *25*, 252-265.

5. Veronesi, M.; Visioli, A. Performance assessment and retuning of PID controllers. *Ind. Eng. Chem. Res.* **2009,** *48*, 2616-2623.

6. Grimholt, C.; Skogestad, S. Optimal PI-control and verification of the SIMC tuning rule. *Proceedings of the IFAC Conference on Advances in PID Control PID;* 2012; pp.

7. Toscano, R. A simple robust PI/PID controller design via numerical optimization approach. *J. Process Control* **2005,** *15*, 81-88.

8. Kim, T.-H.; Maruta, I.; Sugie, T. Robust PID controller tuning based on the constrained particle swarm optimization. *Automatica* **2008,** *44*, 1104-1110.

9. Skogestad, S. Simple analytic rules for model reduction and PID controller tuning. *J. Process Control* **2003,** *13*, 291-309.

10. Gao, X.; Shang, C.; Huang, D.; Yang, F. A novel approach to monitoring and maintenance of industrial PID controllers. *Control Eng. Practice* **2017,** *64*, 111-126.

11. Huang, H.-P.; Jeng, J.-C. Monitoring and assessment of control performance for single loop systems. *Ind. Eng. Chem. Res.* **2002,** *41*, 1297-1309.

12. Srivastava, S.; Misra, A.; Thakur, S.; Pandit, V. An optimal PID controller via LQR for standard second order plus time delay systems. *ISA Trans.* **2016,** *60*, 244-253.

13. Srivastava, S.; Pandit, V. A PI/PID controller for time delay systems with desired closed loop time response and guaranteed gain and phase margins. *J. Process Control* **2016,** *37*, 70-77.

14. Rajapandiyan, C.; Chidambaram, M. Closed-loop identification of second-order plus time delay (SOPTD) model of multivariable systems by optimization method. *Ind. Eng. Chem. Res.* **2012,** *51*, 9620-9633.

15. Ramakrishnan, V.; Chidambaram, M. Estimation of a SOPTD transfer function model using a single asymmetrical relay feedback test. *Comput. Chem. Eng.* **2003,** *27*, 1779-1784.

16. Helbig, A.; Marquardt, W.; Allgöwer, F. Nonlinearity measures: definition, computation and applications. *J. Process Control* **2000,** *10*, 113-123.

17. Gao, X.; Yang, F.; Shang, C.; Huang, D. A review of control loop monitoring and diagnosis: Prospects of controller maintenance in big data era. *Chin. J. Chem. Eng.* **2016,** *24*, 952-962.

18. Chapellat, H.; Bhattacharyya, S. A generalization of Kharitonov's theorem; Robust stability of interval plants. *IEEE Trans. Automat. Control* **1989,** *34*, 306-311.

19. Huang, Y. J.; Wang, Y.-J. Robust PID tuning strategy for uncertain plants based on the Kharitonov theorem. *ISA Trans.* **2000,** *39*, 419-431.

20. Farkh, R.; Laabidi, K.; Ksouri, M. Robust PI/PID controller for interval first order system with time delay. *International Journal of Modelling, Identification and Control* **2011,** *13*, 67-77.

21. Jin, Q.; Liu, Q.; Wang, Q.; Tian, Y.; Wang, Y. PID controller design based on the time domain information of robust IMC controller using maximum sensitivity. *Chin. J. Chem. Eng.* **2013,** *21*, 529-536.

22. Morari, M.; Zafiriou, E. *Robust process control*; Prentice hall Englewood Cliffs, NJ: 1989.

23. Jeng, J. C.; Fu, E. P. Closed-Loop tuning of set-point-weighted proportional-integral-derivative controllers for stable, integrating, and unstable Processes: a unified data-based method. *Ind. Eng. Chem. Res.* **2015,** *54*, 1041-1058.

24. Campi, M. C.; Lecchini, A.; Savaresi, S. M. Virtual reference feedback tuning: a direct method for the design of feedback controllers. *Automatica* **2002,** *38*, 1337-1346.

25. Yang, X.; Xu, B.; Chiu, M.-S. PID controller design directly from plant data. *Ind. Eng. Chem. Res.* **2010,** *50*,

1352-1359.

26. Gao, X.; Yang, F.; Shang, C.; Huang, D. A Novel Data-Driven Method for Simultaneous Performance Assessment and Retuning of PID Controllers. *Ind. Eng. Chem. Res.* **2017,** *56*, 2127-2139.

27. Hast, M.; Aström, K. J.; Bernhardsson, B.; Boyd, S. PID design by convex-concave optimization. *Proceedings of European Control Conference;* Citeseer: 2013; pp 4460-4465.

28. Mercader, P.; Åström, K. J.; Baños, A.; Hägglund, T. Robust PID Design Based on QFT and Convex-Concave Optimization. *IEEE Trans. Control Syst. Technol.* **2016**, 1-12.

29. Yuille, A. L.; Rangarajan, A. The concave-convex procedure. *Neural Comput.* **2003,** *15*, 915-936.

30. Kansha, Y.; Hashimoto, Y.; Chiu, M. S. New results on VRFT design of PID controller. *Chem. Eng. Res. Des.* **2008,** *86*, 925-931.

31. Alfaro, V. M.; Vilanova, R. Robust tuning and performance analysis of 2DoF PI controllers for integrating controlled processes. *Ind. Eng. Chem. Res.* **2012,** *51*, 13182-13194.

32. Jeng, J. C.; Tseng, W. L.; Chiu, M. S. A one-step tuning method for PID controllers with robustness specification using plant step-response data. *Chem. Eng. Res. Des.* **2014,** *92*, 545-558.